Cytoskeleton of living, unstained cells imaged by scanning force microscopy

Leda Chang, Thomas Kious, Max Yorgancioglu, David Keller, and Janet Pfeiffer
Department of Chemistry, and Department of Cell Pathology, School of Medicine, University of New Mexico, Albuquerque, New Mexico 87131 USA

ABSTRACT Subsurface cytoskeletal structure can be visualized in either fixed or living mammalian cells in aqueous medium with ~50 nm resolution using the Scanning Force Microscope (SFM). In living cells, changes in cell topography, or subsurface cytoskeleton caused by the introduction of drugs (colchicine) or cross-linking of surface receptors (by antibodies against IgE bound to the IgE receptor) can be followed in time. Contrast in SFM images of cell surfaces result from both topographic features of the cell and from variations in cell surface "stiffness". The SFM is therefore capable of measuring local compliance and stress in living cells, and so should make it possible to map the cytoskeletal forces used to generate cell motions and changes in cell shape.

INTRODUCTION

All living cells contain a system of fibers and filaments, collectively called the cytoskeleton, by means of which they move, change and maintain shape, effect intracellular movements of organelles, and mechanically divide themselves during mitosis. One of the chief means by which this cytoskeletal network is studied is by light microscopy (in various forms), which allows cytoskeletal networks to be visualized, mapped, and probed in living cells. Recently it has been shown that a new kind of microscope, the Scanning Force Microscope (1), is capable of imaging unstained and live cells in their native environment (2, 3), with resolution considerably higher than can be achieved by light microscopy, (4, 5). The SFM is one example of a larger class of "Scanning Probe Microscopes", including the Scanning Tunneling Microscope (STM), which all operate by scanning a very sharp, sensitive probe tip over the sample surface. In the SFM the tip is mounted on a flexible cantilever so that any forces acting between tip and sample cause a measurable cantilever deflection. The result is a three-dimensional, topographic image that can have very high resolution (for solid samples atomic resolution is common (6, 7), though this has not been achieved on cell surfaces), and can be taken in any liquid, gaseous, or vacuum environment.

Here we investigate the imaging of RBL-2H3 rat leukemic mast cells (RBL cells) by SFM. RBL cells are in vitro model immune system cells which express the high affinity IgE receptor, $F_{\epsilon}R1$. When the Fc receptor binds to the IgE antibody, the cells are sensitized to foreign substances (8). When two or more of these receptor-antibody complexes are cross-linked (by a multivalent antigen) the cell is stimulated and undergoes vast chemical and morphological changes, including tyrosine kinase activation, calcium influx, release of granules containing histamine, heparin, and serotonin, flattening, and large scale changes in the cytoskeleton (8, 10). With the SFM: (*a*) it is possible to observe changes on the surface of living cells when they are stimulated in situ, by introducing drugs or stimulating agents into the sample chamber. (*b*) Upon stimulation of the cell (by cross-linking IgE receptors with IgE and multivalent antigen) it is possible to visualize the cytoskeletal network under the surface of RBL cells. (*c*) It is possible to follow cell movements and changes in the cytoskeletal network with time.

Address correspondence to David Keller.

MATERIALS AND METHODS

To compare SFM imaging with scanning Electron Microscopy, some samples were prepared by critical point drying, even though this is not necessary for the SFM. In these experiments RBL-2H3 cells were placed on 15 mm glass coverslips and activated by incubating for 12 h at 37°C with anti-DNP-IgE contained in Dulbecco's modified Eagle's medium (MEM) with 15% fetal calf serum. The IgE antibodies bind to IgE receptor proteins on the cell surface. When these antibodies subsequently bind to multivalent antigen (the multivalent antigen is DNP-BSA in our case), the receptors are cross-linked and cause stimulation of the cell. The cells were then rinsed with Hank's buffer (10) (125 mM NaCl, 5 mM KCl, 0.64 mM Na_2HPO_4, 0.66 mM K_2HPO_4, 15 mM $NaHCO_3$, 1.7 mM $CaCl_2$, 0.73 mM $MgSO_4$, 10 mM Hepes (pH 7.2), 5.5 mM Dextrose, and 10% BSA), and stimulated by exposure to 1 μg/ml DNP-BSA (in Hank's buffer) at 37°C for a specified period of time. Before imaging they were fixed with 2% glutaraldehyde in 0.1 M cacodylate buffer (0.1 M, pH 7.4) for 30 min, rinsed again with Hank's buffer, then dehydrated with a graded series of ethanol solutions (50, 75, 95, 100%), and finally critical point dried.

In the remaining experiments all cells were imaged in aqueous medium, either alive or after fixation. In both cases the RBL-2H3 cells were allowed to attach to cover slips and incubated with anti-DNP-IgE in the same manner as described above. Cells that were to be fixed were then stimulated with 1.0 μg/ml DNP-BSA for a specified time at 37°C, rinsed in buffer, fixed as for the dried cells above, and stored in phosphate buffer (140 mM NaCl, 10 mM phosphate, pH 7.2) at 4°C. To help determine the nature of the submembranous structure visualized in the SFM, some cells were treated with colchicine (1 μM), for 40 min at 37°C, before being stimulated with DNP-BSA.

Cells that were to be imaged alive were removed from the incubator after activation with anti-DNP-IgE as above, rinsed in Hanks-BSA medium, and placed in the fluid sample cell of the SFM which was filled with Hank's BSA medium at room temperature. The sample was then imaged to locate positions of resting cells. To begin the main experiment the cells were stimulated by injecting 1.0 μg/ml DNP-BSA in

0006-3495/93/04/1282/05 $2.00

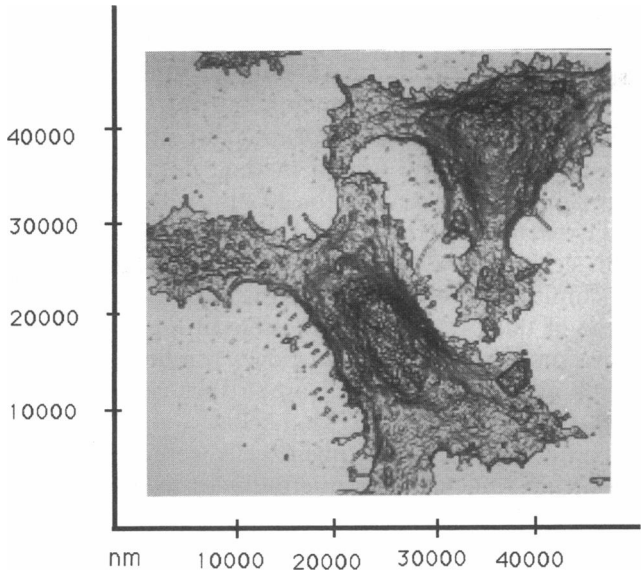

FIGURE 1 Scanning Force Micrograph of two RBL cells stimulated for 5 min with DNP-BSA before fixation. The image is a plot of height versus X-Y position as measured by the SFM probe, displayed as if it were illuminated from above.

Hank's buffer into the fluid cell, and imaged by SFM immediately afterward.

ATOMIC FORCE MICROSCOPY

All samples were imaged with a Nanoscope II Scanning Force Microscope (Digital Instruments, Santa Barbara, CA), with microfabricated silicon nitride cantilevers (Digital Instruments) using a 100 μm "J" scanner. In some cases specially fabricated "electron-beam" SFM tips were used (9) to help reduce sample-tip forces and improve image quality. Imaging forces varied between 10^{-9} and 10^{-8} N, with lower forces used on undried and living cells. All images were taken in height mode.

RESULTS AND DISCUSSION

Fig. 1 is an SFM image of two RBL cells stimulated with DNP-BSA for 5 min, and then prepared in the same way as for imaging in the Scanning Electron Microscope (10), except that the cells were not metal or carbon coated. The image was taken in air at ambient pressure and temperature, and is displayed as an artificially illuminated surface with the illumination from directly above. The SFM image is very similar in appearance to scanning electron micrographs of these cells (10), but contains direct three-dimensional information in addition to the two-dimensional information that is most readily available from light or electron micrographs. In our experience resolution obtained on such samples is usually ~30 nm in the lateral directions and a few nanometers in the vertical direction.

In virtually all our experiments we have found critical point dried cells to differ from undried cells (either fixed or living) in two respects: (*a*) they are flatter at the fringes of pseudopodia and other leading edges, and (*b*) their surfaces appear much rougher. In the first case a typical thickness for a dried pseudopod is ~150 nm (for either stimulated or unstimulated cells), compared to ~1000 nm for unstimulated cells and 300 nm for stimulated cells that were not dried. The flatness is apparently due to collapse of the cell upon drying, despite the care taken to fix important structures and to avoid damage artifacts by critical point drying. In the second case, the roughness on the cell surface is similar to roughness seen in electron micrographs, but, since these cells were not

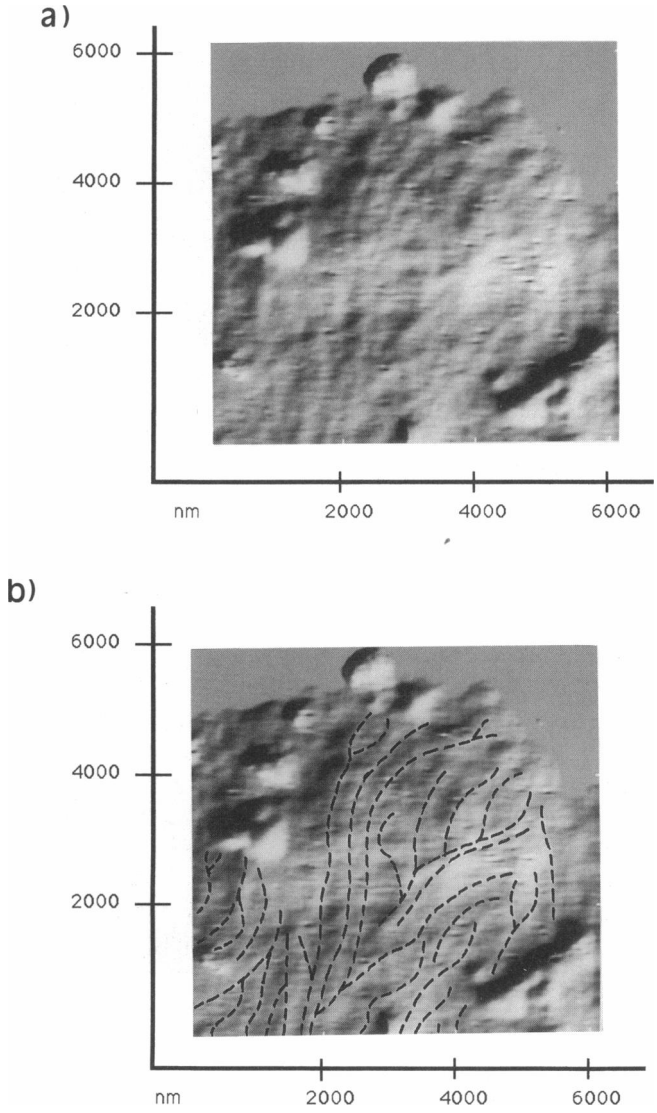

FIGURE 2 (*a*) Scanning Force Microscope image of fixed, stimulated, undried cell in aqueous medium. Cytoskeletal fibers are visible under the membrane. (*b*) Same image as in *a* with major fibers highlighted. The highlighted fibers were determined by comparing the image in *a* with second derivative and surface illumination images.

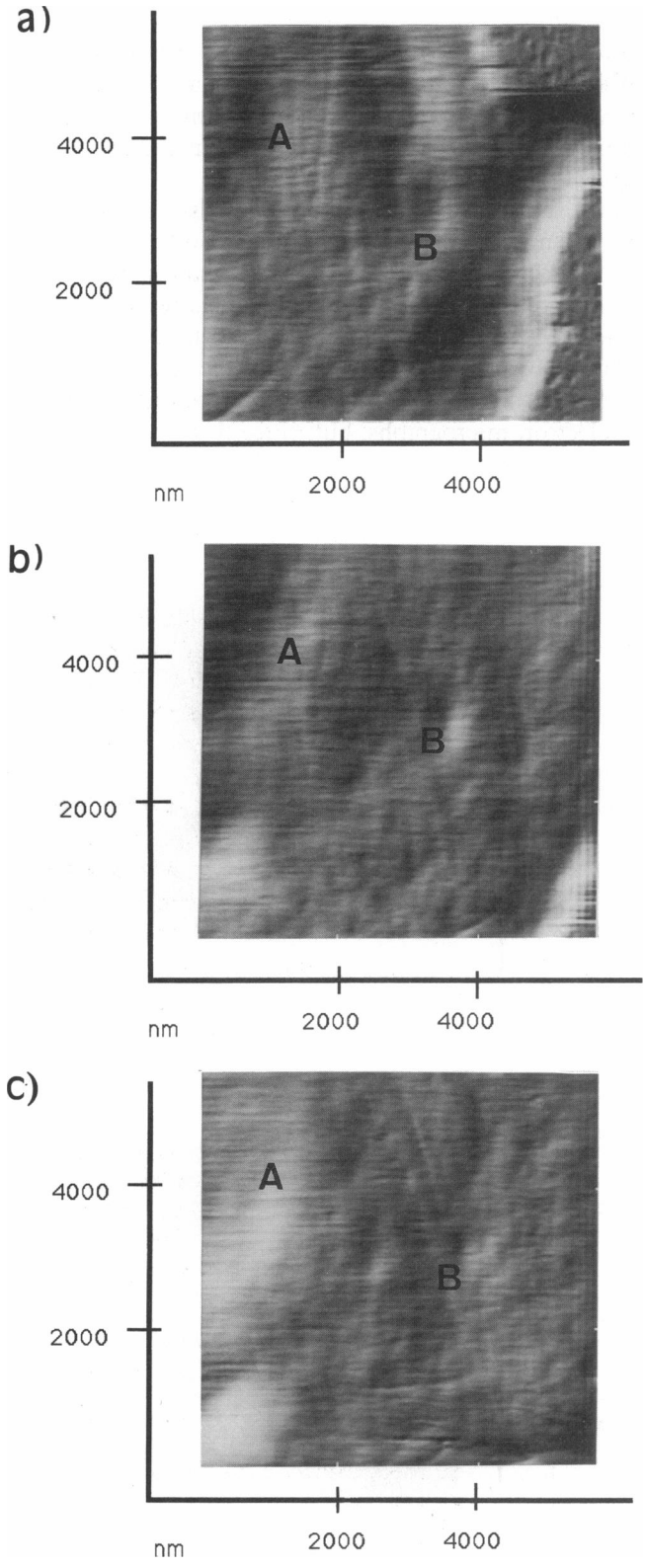

FIGURE 3 SFM images of living cell surfaces. (*a*) Region at the edge of a lamellipod (note the substrate surface along the right side), ~25 min after stimulation with DNP-BSA at 25°C. The derivative of the image has been taken to enhance surface features. (*b*) Same region as in *a* 47 s later. The edge of the lamellipod has moved almost out of the field of view. In the area marked *A* there has been a rise in height and the cytoskeletal fibers have largely disappeared. The high bump in the area marked *B* of *a* has broadened in *b*, and the pattern of cytoskeletal fibers has changed. (*c*) Same region as in *b* 5 min, 4 s later. The edge of the cell is now out of view, area *A* has developed into a very high ridge along the left side of the image, and area *B* has become a broad central bump. The cytoskeletal pattern continues to change.

carbon or metal coated, it must be due to the cell surface itself rather than any coating. A possible explanation is that on dried cells the membrane has been damaged, perhaps by coagulation of membrane proteins.

Fig. 2 *a* and *b*, shows a short pseudopod of a cell that was prepared by the second method described above, that is, it was stimulated (for 20 min with DNP-BSA) and fixed, but not critical point dried. Upon stimulation, RBL cells undergo large morphological changes, with concomitant assembly of cytoskeletal systems (10). Some of this cytoskeleton is visible in Fig. 2 *a*, which shows a system of lines and ridges running under the membrane. Similar networks are also visible in images of live, stimulated cells (see Fig. 3 below).

To help identify these fibers, cells were treated with colchicine, which causes microtubules to disassemble. The cells were prepared in the same way as before and show marked differences from untreated cells. They flatten and extend much less upon stimulation and are much more easily deformed by the SFM probe. However, colchicine treated cells also show cytoskeletal structure similar to that seen in Figs. 2 and 3. Therefore the fibers cannot (all) be microtubules, and are most likely actin assembled to extend the pseudopod (2, 10, 14).

In Fig. 2 *b* the major lines in the network have been highlighted. The cytoskeletal ridges are usually only a few nanometers high, and are not easily visible in the raw grayscale images. Figs. 2 and 3 have been processed to enhance the visibility of surface features, by taking the derivative of the original image. The network shown in Fig. 2 *b* was constructed using Fig. 2 *a* together with the raw grayscale image, second-derivative images, and surface illumination images like Fig. 1. It is not possible to tell from the SFM images whether the branches in the network represent true branches in the underlying cytoskeleton or result from unresolved crossing or merging of fibers. The ability to see these features suggests either that the membrane has become tightly stretched over the cytoskeletal fibers or that as part of the imaging process the SFM tip depresses the unsupported regions of the cell surface between cytoskeletal fibers.

The smallest discernable fibers (in these and other images) appear to be ~50 nm in diameter. This dimension will be affected by at least two factors: (*a*) the size of the probe tip, and (*b*) the effect of the membrane between the tip and the fiber. If the tip shape is known, the effect of tip size can be readily accounted for (6, 7), to give the true profile of the membrane-covered fiber. The electron beam fabricated tips used in these experiments are quite consistently parabolic in shape, with an end

radius of curvature of 10 nm (20 nm diameter). If the cross-sectional profile of the fiber is also approximately parabolic, the general theory shows that the true diameter is just the apparent fiber diameter (measured from the image) minus the tip diameter (11). The smallest visible fibers are then ~30 nm in diameter when corrected for tip effects. The membrane presumably accounts for at least a few nanometers of this, so the true fiber diameter is ~20 nm or less. A single actin filament is 7–10 nm in diameter and microtubules are ~20 nm in diameter, so the smallest resolved features are consistent with small actin bundles or single microtubules. Again, because these fibers are located at the ends of pseudopodia, and because they are still present in colchicine-treated cells, actin bundles are the more likely interpretation.

Images of living, stimulated cells are shown in Fig. 3. We were not able to obtain useful images of unstimulated, living cells. In all attempts to image unstimulated cells the images had a featureless, smeared appearance that we attribute to deformation by the probe tip. Clear images could be obtained within minutes after stimulation, even before much cell flattening had occurred, however, due to the assembly of cytoskeleton and consequent stiffening of the cell. This stiffening of RBL cells (and other cell types) upon stimulation has been observed before (12, 13, 14), using a cantilever arrangement similar in concept to the cantilever of the SFM. By measuring force versus height of the sample (that is, a "force curve") it is possible to make quantitative measurements of the compliance of the cell surface at a single spot as a function of external stimuli and environmental parameters. Our force curves are qualitatively similar to those measured by Liu et al. (14), and we believe this and related force or surface stress measurements may be a major application of the SFM.

The area shown is a region at the advancing edge of a lamellipod of a stimulated cell, and the glass substrate can be seen at the right edge of Fig. 3 *a* and the lower right corner of Fig. 3 *b*. The images were taken in succession, at room temperature, beginning at 25 min after stimulation with DNP-BSA, and show how the state of the cell surface changes with time. Physiological temperature is 37°C, so the cells change more slowly than normal. Fig. 3 *b* was taken at 48 s after Fig. 3 *a*, and Fig. 3 *c* was taken 5 min and 4 s after Fig. 3 *b*. The position of the imaging area was not moved between frames, so the disappearance of the substrate from Fig. 3, *a* to *b*, and again from Fig. 3, *b* to *c*, is due to motion of the cell edge.

The images have been processed to better show cytoskeletal structure, as mentioned above in connection with Fig. 2. In Fig. 3 *a* there is a group of prominent fibers in the upper left (region *A*). In Fig. 3 *b* the fibers in this region are no longer prominent, but a bump in the cell surface has risen by ~20 nm in the same region, as determined by making surface height measurements on the raw SFM images. In Fig. 3 *c* this bump has grown into a prominent feature along the whole left side of the image. A similar progression takes place in the region marked *B*. In Fig. 3 *a* there is a small bump in the right center which grows to a larger bump in Fig. 3 *b*, and finally swells to raise the whole central region of the image in Fig. 3 *c*. In these and other, similar experiments there seem to be a correlation between the appearance of prominent cytoskeletal fibers and the presence or later growth of a bump or small microvillus on the cell surface. It may be that the prominent fibers are those that are especially stiff, that is, are under tension or are contracting, and so are active in causing cell movements at the time the image is taken.

CONCLUSIONS

The SFM can image living cells with resolution considerably higher than light microscopes, and this resolution should improve as the technique develops. There are no fundamental limits until the atomic scale is reached. Since the sample can be kept in its native environment the artifacts caused by drying are avoided. SFM images are true three-dimensional topographs, so that heights, areas, and volumes can be measured directly from raw SFM data. We have shown here that it is possible to observe the distribution and long-time behavior of cytoskeletal fibers in fixed or living cells. If, as suggested by our results, individual cytoskeletal fibers are activated or stressed more than others in the same region, the time sequence of this activation can be followed, and perhaps used to map in detail the kinematics of cellular shape changes and motility.

This work was supported by Research Allocations Committee, Biomedical Research Support Grants, and Sandia-University Research Program grants to D. Keller.

Received for publication 28 September and in final form 3 December 1992.

REFERENCES

1. Binning, G., and C. F. Quate. 1986. Atomic force microscopy. *Phys. Rev. Lett.* 56:930–933.
2. Henderson, E., P. G. Haydon, and D. S. Sakaguchi. 1992. Actin filament dynamics in living glial cells imaged by atomic force microscopy. *Science (Wash. DC)* 257:1944–1946.
3. Häberle, W., J. K. H. Hörber, F. Ohnesorge, D. P. E. Smith, and G. Binnig. 1992. In situ investigations of single living cells infected by viruses. *Ultramicroscopy.* 42–44:1161–1167.
4. Gould, S. A. C., B. Drake, C. B. Prater, A. L. Weisenhorn, S. Manne, H. G. Hansma, P. K. Hansma, J. Massie, M. Longmire, V. Elings, D. Dixon Northern, B. Mukergee, C. M. Peterson, W.

Stoeckenius, T. R. Albrecht, and C. F. Quate. 1990. From atoms to integrated circuit chips, blood cells, and bacteria with the Atomic Force Microscopy. *J. Vac. Sci. Technol. A.* 8:369–373.

5. Horber, J. K. H., W. Haberle, and G. Binning. 1991. Force microscopy in living cells. *J. Vac. Sci. Technol.* B9:1210–1213.
6. Hansma, P., and J. Tersoff. 1987. Scanning tunneling microscopy. *J. Appl. Phys.* 61:R1–R23.
7. Rugar, D., and P. Hansma. 1990. Atomic force microscopy. *Physics Today.* 23–30.
8. Oliver, J. M., J. C. Seagrave, R. F. Stump, J. R. Pfeiffer, and G. R. Deanin. 1988. Signal transduction and cellular response in RBL-2H3 mast cells. *Prog. Allergy.* 42:185–245.
9. Keller, D., and C. C. Chou. 1992. Imaging steep, high structures by scanning force microscopy. *Surface Science.* 268:333–339.
10. Pfeiffer, J. R., J. C. Seagrave, B. H. Davis, G. G. Deanin, and J. M. Oliver. 1985. Membrane and cytoskeletal changes associated with IgE-mediated serotonin release from rat basophil leukemia cells. *J. Cell Biol.* 101:2145–2155.
11. Keller, D. 1991. Reconstruction of STM and AFM images distorted by finite size tips. *Surface Science.* 253:353–364.
12. Petersen, N. O., W. B. McConnaughey, and E. L. Elson. 1982. Dependance of locally measured cellular deformability on position on the cell, temperature and cytochalasin B. *Proc. Natl. Acad. Sci. USA.* 79:5327–5331.
13. Pasternak, C., and E. L. Elson. 1985. Lymphocyte mechanical response triggered by cross-linking surface receptors. *J. Cell Biol.* 100:860–872.
14. Z. Liu, J. Young, and E. L. Elson. 1987. Rat basophil leukemia cells stiffen when they secrete. *J. Cell Biol.* 105:2933–2943.